HHS Public Access

Author manuscript

Int J Med Microbiol. Author manuscript; available in PMC 2021 November 20.

Published in final edited form as:

Int J Med Microbiol. 2021 May ; 311(4): 151511. doi:10.1016/j.ijmm.2021.151511.

Strain and host-cell dependent role of type-1 fimbriae in the adherence phenotype of super-shed *Escherichia coli* O157:H7

Robab Katani[a,1], **Indira T. Kudva**[b,**,1], **Sreenidhi Srinivasan**[a], **Judith B. Stasko**[d], **Megan Schilling**[a], **Lingling Li**[e], **Rebecca Cote**[a], **Chitrita DebRoy**[e], **Terrance M. Arthur**[f], **Evgeni V. Sokurenko**[g], **Vivek Kapur**[a,c,*]

[a]The Huck Institutes of the Life Sciences, Pennsylvania State University, University Park, PA, USA

[b]Food Safety and Enteric Pathogens Research Unit, National Animal Disease Center, Agricultural Research Service, U.S. Department of Agriculture, Ames, IA, USA

[c]Department of Animal Science, The Pennsylvania State University, University Park, PA, USA

[d]Microscopy Services, National Animal Disease Center, Agricultural Research Service, U.S. Department of Agriculture, Ames, IA, USA

[e]Department of Veterinary and Biomedical Sciences, The Pennsylvania State University, University Park, PA, USA

[f]Roman L. Hruska U.S. Meat Animal Research Center, Agricultural Research Service, U.S. Department of Agriculture, Clay Center, NE, USA

[g]Department of Microbiology, University of Washington, Seattle, WA, USA

Abstract

Super-shed (SS) *Escherichia coli* O157 (*E. coli* O157) demonstrate a strong, aggregative, locus of enterocyte effacement (LEE)-independent adherence phenotype on bovine recto-anal junction squamous epithelial (RSE) cells, and harbor polymorphisms in non-LEE-adherence-related loci,

[*]Corresponding author at: The Huck Institutes of the Life Sciences, Pennsylvania State University, University Park, PA, USA. vkapur@psu.edu (V. Kapur). [**]Corresponding author at: Food Safety and Enteric Pathogens Research Unit, National Animal Disease Center, Agricultural Research Service, U.S. Department of Agriculture, Ames, IA, USA. Indira.kudva@usda.gov (I.T. Kudva).

Author Contributions

Conceptualization: Vivek Kapur, Robab Katani, Indira T. Kudva.

Data Curation: Robab Katani, Indira T. Kudva, Rebecca Cote, Megan Schilling.

Investigation and experiment performance: Robab Katani, Indira T. Kudva, Lingling Li, Sreenidhi Srinvasan, Judith B. Stasko, Chitrita Debroy, Terrance M. Arthur.

Formal Analysis: Robab Katani, Indira T. Kudva.

Funding acquisition: Vivek Kapur, Indira T. Kudva, Evgeni V. Sokurenko.

Methodology: Vivek Kapur, Robab Katani, Indira T. Kudva, Evgeni V. Sokurenko.

Visualization: Robab Katani, Indira T. Kudva, Judith B. Stasko, Rebecca Cote.

Writing – original draft: Robab Katani, Indira T. Kudva.

Writing – reviewing & editing: Vivek Kapur, Robab Katani, Indira T. Kudva, Lingling Li, Sreenidhi Srinvasan, Megan Schilling, Judith B. Stasko, Rebecca Cote, Terrance M. Arthur, Evgeni V. Sokurenko, Chitrita DebRoy.

[1]These authors contributed equally to this work.

Declaration of Competing Interest

The authors have declared that no competing interest exists.

Appendix A. Supplementary data

Supplementary material related to this article can be found, in the online version, at doi:https://doi.org/10.1016/j.ijmm.2021.151511.

including in the type 1 fimbriae operon. To elucidate the role of type 1 fimbriae in strain- and host-specific adherence, we evaluated the entire Fim operon (FimB-H) and its adhesion (FimH) deletion mutants in four *E. coli* O157 strains, SS17, SS52, SS77 and EDL933, and evaluated the adherence phenotype in bovine RSE and human HEp-2 adherence assays. Consistent with the prevailing dogma that *fimH* expression is genetically switched off in *E. coli* O157, the *ΔfimH*SS52, *ΔfimB-H*SS52, *ΔfimB-H*SS17, and *ΔfimH*SS77 mutants remained unchanged in adherence phenotype to RSE cells. In contrast, the *ΔfimH*SS17 and *ΔfimB-H*SS77 mutants changed from a wild-type strong and aggregative, to a moderate and diffuse adherence phenotype, while both *ΔfimH*EDL933 and *ΔfimB-H*EDL933 mutants demonstrated enhanced binding to RSE cells ($p < 0.05$). Additionally, both *ΔfimH*SS17 and *ΔfimH*EDL933 were non-adherent to HEp-2 cells ($p < 0.05$). Complementation of the mutant strains with their respective wild-type genes restored parental phenotypes. Microscopy revealed that the SS17 and EDL933 strains indeed carry type 1 fimbriae-like structures shorter than those seen in uropathogenic *E. coli*. Taken together, these results provide compelling evidence for a strain and host cell type-dependent role of *fimH* and the *fim* operon in *E. coli* O157 adherence that needs to be further evaluated.

Keywords

Escherichia coli ; O157:H7; Type-1 fimbriae; Super-shedder; FimH

1. Introduction

Shiga toxin-producing *Escherichia coli* O157:H7 (*E. coli* O157) is a zoonotic foodborne pathogen, and the source of many recent outbreaks associated with the consumption of under-cooked meat and contaminated leafy green vegetables (Dewey-Mattia et al., 2018; Furukawa et al., 2018; Mikhail et al., 2018; Tamminen et al., 2018). In the US alone, *E. coli* O157 accounts for close to 80,000 infections yearly, and can present broad clinical spectrum of symptoms ranging from bloody diarrhea to hemorrhagic colitis, and severe life-threatening complications such as hemolytic uremic syndrome (HUS) (Centers for Disease Control and Prevention, 2011; Gyles, 2007; Nataro and Kaper, 1998; Paton and Paton, 1998; Scallan et al., 2011).

Asymptomatic cattle are the primary reservoir of *E. coli* O157, and colonized animals harbor the organism at the terminal recto-anal junction (RAJ) of the intestinal tract (Lim et al., 2007). RAJ is a region between the lymphoid follicle-associated columnar epithelial (FAE) cells and stratified squamous epithelial (RSE) cells found towards the anal canal. *E. coli* O157 typically localize in the RAJ, whereas other Shiga toxin-producing *E. coli* (STEC) serotypes are found throughout the large intestine (Lim et al., 2007; Kudva and Dean-Nystrom, 2011; Naylor et al., 2003).

A small subset of colonized cattle, termed as “super-shedder (SS)”, excrete *E. coli* O157 at extremely high levels ($\geq 10^4$ CFU/g of feces) and epidemiological studies show that >96 % of *E. coli* O157 isolates can originate from 10 % of the SS animals on a farm (Naylor et al., 2003; Arthur et al., 2010; Omisakin et al., 2003). Mathematical models predict that the presence of SS animals on farms are key contributors to the high transmission rates of *E.*

coli O157 despite having a low within-herd prevalence (Naylor et al., 2003; Matthews et al., 2006; Stevens et al., 2002).

Previously, we reported that super-shed *E. coli* O157 (SS- *E. coli* O157) strains exhibit a non-locus of enterocyte effacement (LEE)- related, strong and aggregative adherence (hyper-adherence) phenotype on bovine recto-anal junction squamous epithelial (RSE) cells that is distinct from the moderately aggregative phenotype observed with the EDL933 strain of *E. coli* O157 (Cote et al., 2015;). However, the molecular mechanisms contributing to this phenotype, in particular in SS- *E. coli* O157 strains, remain unknown. Recently, we sequenced and closed the genomes of two SS- *E. coli* O157 strains, SS17 (Cote et al., 2015) and SS52 (Katani et al., 2015) and performed draft sequencing of SS77. The comparative genomic analyses revealed that SS- *E. coli* O157 isolates may have greater genetic identity with reference *E. coli* O157 strains than amongst themselves (Katani et al., 2017). Our analysis did not identify any evidence of shared pattern of substitutions, including in adherence-related loci amongst the SS- *E. coli* O157 strains, although polymorphisms in non-LEE-dependent adherence related loci, including in the type 1 fimbriae operon, were observed (S1A and S1B Figs.) (Cote et al., 2015; Katani et al., 2017).

Knowing type 1 fimbria are considered as not expressive in *E. coli* O157 and the existed nsSNPs in the operon, we were curious about: 1) if this operon is actually not being expressed in *E. coli* O157, 2) if it is not being expressed, does it play another role in the adherence of the *E. coli* to the host cells, and 3) does *E. coli* O157 supershedders adhere differently to different host cells? Overall, our current study sought to better understand the molecular basis of the hyper-adherence phenotype observed in SS- *E. coli* O157 strains in the context of the type 1 fimbriae and the EDL933 strain of *E. coli* O157.

2. Materials and methods

2.1. Bacterial strains

Two fully sequenced strains, SS17 [NZ_CP008805] and SS52 [CP010304] (Cote et al., 2015; Katani et al., 2015), and a draft genome of an additional strain SS77 [PRJNA650142], were used as representative SS- *E. coli* O157 isolates, based on their genotypic and phenotypic features commonly found in other SS- *E. coli* O157 isolates, as well as in strains associated with human illnesses (Arthur et al., 2013; PulseNet, 2021). EDL933 [NC_002655], a well-studied *E. coli* O157 strain, was used as a reference strain for comparative analyses (Burland et al. (1998); Perna et al. (2001a)). *E. coli* O157 strains Sakai [NC_002695], TW14359 [NC_013008], and EC4115 [NC_011353] were also used as reference genomes for comparative analyses (Eppinger et al. (2011); Hayashi et al., 2001; Kulasekara et al., 2009; Perna et al., 2001b). Uropathogenic *E. coli* (UPEC) strain CFT073 [NC_004431] and *E. coli* HB101 (A Hybrid of *E. coli* K12 and *E. coli* B) were used as positive and negative controls for all fimbrial assays.

2.2. Antisera

Polyclonal rabbit antisera containing antibodies targeting the lectin (Pab280) and pilin (A-PD) domains of FimH were used as primary antisera in immunostaining experiments

targeting the type 1 fimbriae. The primary antisera were incubated with the FimH-knock-out mutants (SS17Δ*fimH* and EDL933Δ*fimH*) constructed for this study to increase specificity to FimH domains and prevent cross-reaction with other fimbrial structures. Sera absorption was done as previously described with slight modification (John et al., 2005). The anti-lectin and anti-pilin antisera were separately incubated with in vitro grown (LB broth, 37 °C) and mixed SS17Δ*fimH* and EDL933Δ*fimH* cultures. The sera were sequentially absorbed with unheated and heat inactivated (100 °C) bacterial cell pellets and absorbed sera stored at − 80 °C until further use.

Polyclonal rabbit antisera generated against the curli subunit protein curlin/CsgA, obtained from Jorge A. Giron, University of Virginia, Charlottesville, VA., was included to distinguish the type 1 fimbrial structures from curli fimbriae, and verify the specificity of the absorbed anti-FimH domain antisera. Goat anti-rabbit IgG (H + L) antibody tagged with 6 nm gold particles were used as secondary antisera.

2.3. Design of molecular constructs

Single step inactivation of the type 1 fimbriae operon (*fimB-H*) and its encoded adhesin (*fimH*) was performed using previously described methods (Cote et al., 2015; Datta et al., 2006). Briefly, using the pKD4 plasmid and PCR, a kanamycin resistance (KanR) cassette was generated with arms of homology to the gene/operon of interest. Recombination was facilitated with pKD119 (pBAD-λ RED) via electroporation followed by treatment with arabinose, electroporation with the KanR cassette, and selection using LB supplemented with 50 μg/mL kanamycin. The insertion and location of the KanR cassette were confirmed by PCR and sequencing. Kanamycin was removed via pCP20 transformation and validated using Kan30 plates, colony PCR, and sequencing (S1 Table).

2.4. Complementation

Complementation of SS17 and EDL933 *fimH* deletion mutants was performed using pBBR1MCS-encoded *fimH* as previously described (Kovach et al., 1995). Briefly, *fimH* was amplified from SS17 genomic DNA with appropriate restriction sites added to the forward and reverse primers (S2 Table). This gene of interest was inserted into the multiple cloning site (MCS) of pBBR1MCS by restriction enzyme cloning in Max Efficiency DH5α competent cells (Life Technologies, Inc.) and selection was done on LB supplemented with 15 μg/mL gentamycin. The transformants obtained following blue-white screening were verified for the presence of the insert in the correct orientation using PCR and sequence analysis. The positive clone was used to extract plasmid DNA, which was then transformed into Δ *fimH* EDL933 and Δ *fimH* SS17. The original knockouts and complementary strains constructed in this study are listed in the S2 and S3 Tables.

2.5. Eukaryotic cell adherence assay

2.5.1. RSE cells—

E. coli O157 strains were cultured overnight in Dulbecco Modified Eagle Medium-Low Glucose (DMEM; Gibco/Invitrogen Corporation, Grand Island, NY) at 37 °C without aeration, pelleted, and re-suspended in DMEM-No Glucose (DMEM-NG) as previously described (Cote et al., 2015; Kudva et al., 2017). RSE cells were obtained from rectoanal junction swabs or necropsy tissues of healthy cattle as previously described (Cote

et al., 2015; Kudva et al., 2017). RSE cells were suspended in 1 mL DMEM–NG to a final concentration of 10^5 cells/mL, and the bacteria were mixed with RSE cells to achieve a final bacteria to cell ratio of 10:1. After 4 h of incubation at 37 °C with shaking, the mixture was pelleted, washed, and reconstituted in 100 μl of dH_2O. Drops of the suspension (2 μl) were placed on Polysine (Thermo Scientific Pierce, Rockford, IL) slides and dried overnight under direct light to quench nonspecific fluorescence. Then they were fixed in cold 95 % ethanol for 10 min. The slides were stained with 0.6 % Giemsa stain (Sigma), or with fluorescence-tagged antibodies specific to the *E. coli* O157 antigen and cytokeratins of the RSE cells, and adherence patterns on RSE cells were recorded, qualitatively-quantitatively as previously described (Cote et al., 2015). Adherence patterns were qualitatively recorded as diffuse, aggregative, or non-adherent and quantitated using percent of RSE cells with or without adhering bacteria (Kudva et al., 2012); strongly adherent when more than 50 % of RSE cells had >10 adherent bacteria, moderately adherent when 50 % or less of the RSE cells had 1–10 adherent bacteria and non-adherent when less than 50 % of the RSE cells had only 1–5 adherent bacteria (Kudva et al., 2012). Quantitative data was evaluated for statistical significance against data from wild-type strains (2-tailed, unpaired t-test; $p < 0.05$) (GraphPad Prism version 8.0.0, GraphPad Software, San Diego, CA)

2.5.2. HEp-2 cells—HEp-2 cells (Human epidermoid carcinoma of the larynx cells with HeLa contamination; ATCC CCL-23; American Type Culture Collection, Manassas, VA) were used in place of RSE cells for comparative purposes. *E. coli* O157 adherence pattern on HEp-2 cells was determined using the same assay conditions used for the RSE adherence assay above. Slides were stained with fluorescence-tagged antibodies that target the *E. coli* O157-antigen and the HEp-2 cell actin filaments and adherence recorded as described for RSE cells above (Cote et al., 2015; Kudva et al., 2017).

2.6. Transmission electron microscopy (TEM)

2.6.1. Culture conditions—Bacteria were grown at 37 °C for 18 h under static and aerobic conditions and passaged for ten days in BHI broth (Gentamicin was added for the complemented strains). The 10- day cultures were stored at room temperature for 24 h, gently centrifuged (400 × *g*), and the bacterial pellets used for TEM.

2.6.2. Negative staining—10μl of each bacterial pellet suspension was placed separately on dental wax, and copper 200 mesh formvar coated grids and placed into (floated in) each of the suspension for 1 min. Grids were gently wicked and placed in 0.1 % phosphotungstic acid (PTA, pH 7) for 10 s, fixed in Karnovsky's solution (2% paraformaldehyde/2.5 % glutaraldehyde) for 1 min, and gently wicked and dipped in saline followed by distilled water. Dried grids were visualized on the FEI TecnaiTM G2 Biotwin electron microscope at the National Animal Disease Center/USDA, Ames, Iowa, or stored at RT in a desiccator until ready to view.

2.6.3. Immuno-gold staining—Additional grids were prepared from each bacterial pellet as described above but without negative staining with PTA. The fixed grids were washed in 0.05 M Tris with 0.05 % Tween 20 (Tris-T) for 10 min followed by etching in saturated solution of sodium metaperiodate for 15 min (Stirling and Graff, 1995). Etching

was done to improve the detection of pilin and lectin domains in the midst of curli fibers. To Post-etch the grids, they were rinsed in Tris-T and blocked with 5% bovine serum albumin (BSA) in Tris for 30 min. Primary antibody dilutions were prepared in Tris-T with 0.1 % BSA (TBT) as follows: 1:20 dilution for anti-pilin and anti-lectin antisera, and 1:80 dilution for anti-curli antisera. Grids were incubated in primary antibody dilution, post-blocking for 60 min. Negative control grids were incubated in TBT only. Grids were rinsed in TBT and incubated with gold-tagged secondary antibody, diluted 1:20 in TBT, for 60 min. Subsequently, the grids were washed with TBT and distilled water, dried on filter paper, and visualized on the FEI TecnaiTM G2 Biotwin electron microscope at the National Animal Disease Center/USDA, Ames, Iowa, or stored at RT in a desiccator ready to view.

2.7. Agglutination assay of SS strains

Yeast and guinea pig red blood cell agglutination assays were performed to evaluate the production of type I fimbriae by the SS- *E. coli* O157 strains. The evaluation of type I fimbriae production was measured using yeast agglutination as described previously (Garcia--Contreras et al., 2008). Briefly, 10 strains of SS- *E. coli* O157 were grown on Luria broth (LB) plates overnight, and single colonies inoculated into liquid LB broth and grown for 48 h at 37 °C under static conditions. Cells were harvested and concentrated in 1X PBS to reach OD_{600} of ~ 0.5. The bacterial cells were then mixed with an equal volume of 10 % W/V suspension of brewer's yeast (ACROS Organics, catalog # AC36808–0010) in 1X PBS in the presence and absence of 3% D (+) α-mannose. 20 mL of the mixture was poured onto microscope glass slides and the yeast agglutination was evaluated after 3−5 min. Two strains, *E. coli* K12 BW25113 Δ*fimA*-Kan 50 mg/mL (negative control) and *E. coli* K12 AG1/pCA24N-*fimA*-Cm 30 mg/mL (positive control), were used, which were kind contributions of Dr. Thomas Wood from Penn State. Agglutination was also evaluated in 10 % guinea pig RBC (Innovative Research) using the same procedure.

3. Results

3.1. Comparative genomic analysis of the type 1 fimbriae operon reveals several nonsynonymous Single Nucleotide Polymorphisms (nsSNPs) amongst E. coli O157 strains

It is well documented that in enterohemorrhagic *E. coli* (EHEC), including *E. coli* O157, a 16 bp deletion in the *fimA* promoter region prevents the inversion of the fim switch to the "on" orientation, and thus type 1 fimbriae are not expressed (Iida et al., 2001; Li et al., 1997; Roe et al., 2001). Our recent comparative genomic analyses revealed that, like what has been previously described in other *E. coli* O157 strains, the *fimB/fimE* switch in both SS17 and SS52 is in the "off" orientation. Additionally, both strains harbor the 16-bp deletion 352 bp upstream of *fimA* and fully conserved type 1 *fim* operon regulatory loci including Leucine-Responsive Regulatory Protein (LrP), Integration host factors (IHFA-B), and DNA-binding transcriptional dual regulator (HNS) (Cote et al., 2015; Katani et al., 2015, 2017; Li et al., 1997; Gally et al., 1993; Klemm, 1984).

Our previous investigations in cell assays noted no differences in adherence of strain SS17 to RSE or to HEp-2 cells in the presence or absence of D + Mannose, a finding that has been recently corroborated by evidence that none of the SS- *E. coli* O157 isolates

tested agglutinated yeast or guinea pig red blood cells (RBCs) under conditions favorable for fimbrial expression. This suggested that factors other than type I fimbriae may be responsible for the hyper aggregative adherence phenotype of SS- *E. coli* O157 strains on bovine RSE cells (Cote et al., 2015). Surprisingly, however, detailed comparative genomic analyses of the *fim* operon in SS52 with *E. coli* O157 reference strains revealed the presence of several non-synonymous single nucleotide polymorphisms (nsSNPs). These nsSNPs included, a nsSNP (V1M) in both *fim*E and *fim*C across all the reference strains, a nsSNP in *fimB* (P80S) in comparison with TW14359, and a nsSNP in *fimA* (A100 V) in comparison with Sakai (Table 1).

Our analysis also indicated that *fimI* (fimbrial protein) encodes for a protein with varying amino acid lengths in different *E. coli* O157 strains. In SS52, *fimI* encodes for 179 amino acids (identical to TW14359), whereas, in EDL933, Sakai, and SS17, this gene encodes for 215 amino acids matching the last 179 amino acids in the C-terminus of the SS52. In EC4115 the gene encodes for 165 amino acids, missing the first 14 amino acid at the N terminus of the SS52 *fimI* (Fig. 1).

Hyperallelic variation of *fimH* is one the most studied pathoadaptive mutations in *E. coli* (Sokurenko et al., 1998, 1992; Sokurenko et al., 1994). For example, A27 V FimH polymorphism has been previously reported to be pathoadaptive for *E. coli* (Sokurenko et al., 1998), and the N135 K FimH mannose-binding pocket mutation is found in EHEC strains (Shaikh et al., 2007). We also observed the N135 K nsSNP in *fimH* in both Sakai and EDL933 in comparison with the rest of the reference genomes, and nsSNP (A27 V) was also found in *E. coli* str. K-12 substr. MG1655 (CP009685) in comparison with *E. coli* O157 reference strains (S2 Fig.).

3.2. E. coli SS-O157 and EDL933 strains exhibit distinct adherence patterns on bovine and human epithelial cells

Given the nsSNPs in EDL933 and Sakai in comparison with other reference *E. coli* O157 strains, the host pathoadaptive nature of *fimH* in some species, and the striking differences in adherence between SS and non-SS isolates to bovine recto-anal junction squamous epithelial (RSE) cells (Cote et al., 2015), we used a molecular genetic approach to assess the role of the Type 1 fim operon in this adherence. We knocked out either the entire type 1 fim operon (*fimB-H*) or its adhesin gene (*fimH*) in three SS- *E. coli* O157 (SS17, SS52, and SS77) strains and the EDL933 *E. coli* O157 strains, and evaluated their adherence to bovine RSE and human HEp-2 epithelial cells.

The results showed no differences in the adherence characteristics of SS17Δ*fimB-H* and SS52Δ*fimB-H* on RSE cells; however, the adherence characteristics of SS77Δ*fimB-H* changed from aggregative and strong- observed in the parental SS77 strain- to diffuse and moderate in the mutant ($p = 0.0102$) (Figs. 2 and 3, and S3 Fig, and S4 and S5 Tables). The EDL933Δ*fimB-H* mutant presented an aggregative, strong adherence pattern (similar to wild type SS- *E. coli* O157 strains) as compared to the aggregative, moderate phenotype observed with the parental strain on RSE cells ($p = 0.0463$). No differences were observed in the adherence patterns of SS17Δ*fimB-H*, SS52Δ*fimB-H*, SS77Δ*fimB-H*, and

EDL933Δ*fimB-H* mutants on HEp-2 cells compared to their parental strains, each exhibiting a diffuse, moderate adherence phenotype (Figs. 2 and 3, and S4 and S5 Tables).

We next examined the role, if any, of the major pathoadaptive adhesins associated with FimH, on the adherence patterns of the SS-*E. coli* O157 and EDL933 strains of *E. coli* O157 on RSE and HEp-2 cells. In striking contrast to the aggregative, strong adherence phenotype of SS17 on RSE cells, the SS17Δ*fimH* mutant showed a diffuse, moderate adherence phenotype on RSE ($p = 0.0028$) and a non-adherent phenotype on HEp-2 cells ($p = 0.0306$) (Figs. 2 and 3, and S3 Fig). However, similar to what was seen in the case of the *fim* operon mutants, this effect on the adherence phenotype was not conserved amongst the other SS isolates tested, as no differences from the wild-type strains were observed in the adherence phenotype of SS77Δ*fimH* and SS52Δ*fimH* to either RSE or HEp-2 cells. Unexpectedly, the results revealed an increased adherence phenotype in the EDL933Δ*fimH* mutant ($p= 0.0225$) on RSE cells, similar to what was observed with the EDL933Δ*fimB-H* mutant (Figs. 2 and 3, and S3 Fig). In addition, EDL933Δ*fimH* was non-adherent on HEp-2 cells ($p = 0.0072$) (Figs. 2 and 3, and S3 Fig, and S4 and S5 Tables).

3.3. Complementation of fimH mutations restores the wild type phenotype

FimH complemented strains of SS17 and EDL933 were constructed and were evaluated using the adherence assay (S2 and S3 Tables). The results show that complementation with the *fimH*-encoding plasmid fully restored the wild type adherence phenotype (to aggregative, strong in SS17 and aggregative, moderate in EDL933) in RSE cells, confirming that the *fimH* gene likely plays a role in the adherence phenotype of *E. coli* O157 strains to specific mammalian cells (Figs. 4 and S4 Fig). Similarly, the adherence phenotype in the deletion mutants of SS17 and EDL933 was restored to diffuse moderate on human HEp-2 cells when complemented with the plasmid containing the wild-type sequence (Figs. 4 and S3–5 Figs, and S6 and S7 Tables).

3.4. Type 1 fimbriae-like appendages are present on E. coli O157 strains SS17 and EDL933 as verified by transmission electron microscopy

To visually confirm the presence of type 1 fimbriae-like structures in the tested strains, negative staining electron microscopy was performed on wild type SS17, wild type EDL933, and Δ*fimH* and Δ*fimH*-complemented strains of SS17 and EDL933. Our results indicated that both wild type SS17 and EDL933 strains indeed carry fimbriae-like structures (Fig. 5A) that are shorter and denser than what is seen in the uropathogenic *E. coli* (UPEC) CFT073 strain used as a positive control. Electron micrographs showed no visible fimbriae-like structures in SS17Δ*fimH* and EDL933Δ*fimH* mutants, although more flagellated cells were observed in both (Fig. 5B). When the strains were complemented, the fimbrial phenotype was restored in both cases (Fig. 5C).

For further characterization, all bacterial strains and their mutant derivatives were stained with primary antibodies targeting the pilin and lectin domains of FimH, and a gold-tagged secondary antibody. The anti- curlin (CsgA) primary antibody was also included to distinguish the type 1fimbriae-like structures from curli fimbriae. As clearly seen with the control UPEC strain, the anti-FimH antibodies stained structures distinct from those targeted

by the anti-CsgA antibody (Fig. 6A). No nonspecific binding of the gold-tagged secondary antibody was observed to bacteria in the negative control grids, incubated only with the secondary antibody and not any of the primary antibodies, further confirming the specificity of the labelling by the antibodies targeting FimH (Fig. 6A).

The anti-FimH antibodies also labelled the type 1 fimbriae-like structures in wild type SS17, wild type EDL933, and Δ*fimH*-complemented strains of SS17 and EDL933 (Fig. 7A–B). No staining was observed with SS17Δ*fimH* and EDL933Δ*fimH* mutants and the a-fimbrial control *E. coli* HB101strain (Figs. 7A–B and 6 B).

4. Discussion

Despite the considerable impact of super-shedding on the transmission of *E. coli* O157 within cattle herds, the mechanism by which *E. coli* O157 strains from super-shedder cattle colonize their bovine hosts remains largely unknown. This knowledge is essential for the development of rational approaches to control SS- *E. coli* O157 infections in cattle and prevent their transmission through the food chain to humans, especially due to evidence that reduction in the adherence and colonization of *E. coli* O157 leads to a decrease in the spread of the pathogen amongst cattle, reducing the risk of transmission to humans (Naylor et al., 2003; Stevens et al., 2002).

Our previous studies showed that wild type SS- *E. coli* O157 strains manifest a LEE-independent, aggregative, strong adherence to RSE cells and a diffuse moderate adherence to the HEp-2 cells (Cote et al., 2015). Genomic comparisons between two strains of SS- *E. coli* O157 with other well-defined strains of *E. coli* O157 confirmed the genetic heterogeneity amongst *E. coli* O157 strains (S1B Fig) (Katani et al., 2017). Recent investigations also suggest that there is considerable genetic heterogeneity amongst *E. coli* O157 strains recovered from SS cattle, and no common genotype in *E. coli* O157 can be specifically associated with super-shedding in cattle (Arthur et al., 2013). In our analysis, we observed some key polymorphisms in SS- *E. coli* O157 and reference *E. coli* O157 strains and decided to explore the non-LEE virulence factors associated with adherence of *E. coli* O157 to host cells. Type 1 fimbrial operon carries several nsSNPs amongst the *E. coli* O157 strains and this operon has largely been unexplored due to the prevailing dogma of the operon not being expressed in *E. coli* O157. We decided to take a closer look at the operon, specifically the adhesin *fimH*, adhesin located at the tip of the fimbrial shaft (Abraham et al., 1987; Brinton, 1965; Hanson et al., 1988; Klemm and Christiansen, 1987). We used a molecular genetic approach and constructed a series of mutants to assess the role of the entire type 1 fimbrial operon (*fimB-H*) and the *fimH* gene in the adherence of three SS- *E. coli* O157 strains (SS17, SS52, and SS77), and a well-characterized *E. coli* O157 strain EDL933; we evaluated the adherence of the wild type, Δ*fimB-H*, and Δ*fimH* mutants to the bovine RSE and human HEp-2 epithelial cells.

Contrary to the prevailing dogma of a limited role for type 1 fimbriae in the pathogenesis of *E. coli* O157 infection based on human *in vitro* and mouse *in vivo* models, our results showed that type 1 fimbriae may play a role in *E. coli* O157 adherence to the host cells and that this adherence is strain and host-cell type dependent (Farfan et al., 2013; Jordan et al.,

2004; Lloyd et al., 2012). Deletion of the *fim* operon had a divergent role on the adherence of some (SS77 and EDL933), but not all *E. coli* O157 strains (SS17 and SS52), and the expressed phenotype was dependent on the type of the host cell (RSE versus HEp-2 cell). The results also indicated that deletion of *fimH* alone (but not the entire *fim* operon) results in a non-adherent phenotype of both EDL933 and SS17 on HEp-2 cells, suggesting that the regulation of the expression of *fimH* is essential for both SS17 and EDL933 adherence to HEp-2 cells, and that the expression of these elements is host cell dependent.

On the other hand, our data showed that deletion of either the entire *fim* operon (Δ*fimB-H*) or *fimH* in EDL933 enhances the adherence pattern phenotype of EDL933. Interestingly, EDL933Δ*fimH* exhibited a non-adherent phenotype on HEp-2 cells as contrasted with the diffuse moderate phenotype of the parental and EDL933Δ*fimB-H* strains (Figs. 2 and 3, and S3 Fig.). These results provide evidence for a role of both the fim operon and *fimH* in the adherence phenotype of some, but not all strains of *E. coli* O157, including SS-*E. coli* O157 isolates. Furthermore, the striking heterogeneity observed in the adherence phenotypes of the Δ*fimB-H* and Δ*fimH* mutants of SS17 to both RSE and HEp-2 cells and the Δ*fimH* mutant of EDL933 on HEp-2 cells also provides strong evidence for the presence of complex regulatory networks and multiple factors that are involved in the expression of the adherence phenotype of SS and other *E. coli* O157 strains to mammalian cells.

The change in EDL933 phenotype seen with the deletion of either the entire *fim* operon or *fimH* to a phenotype similar to a SS isolate on RSE cells was striking, and suggests that despite the presence of the switch deletion in EDL933 *fim* that would predict that the gene is not transcribed, its presence in the genome has a suppressive effect on the expression of other factors that result in the hyper-adherent phenotype of EDL933 on RSE cells. What these data also suggest is that the aggregative strong adherence of *E. coli* O157 to bovine RSE cells may perhaps be inducible, and that potential suppressor element(s) associated with *fimH* and the *fim* operon are, at least in part, responsible for the repression of this phenotype in EDL933. To confirm the specificity of the observed phenotypes in the deletion mutants in the adherence of *E. coli* O157 strains and fulfill molecular Koch's molecular postulates, a series of *fimH* complementation strains of SS17 and EDL933 were constructed (Supplemental Table 2, S4 Fig.). The adherence phenotypes of the deletion mutants in SS17 and EDL933 were restored in both *fimH* and *fimB-H* complemented strains. These results suggest that despite the *fim* switch being permanently turned "off" in O157, additional genetic elements located in the region encoding *fimH* likely permit a regulatory override of this switch, and the existence of a complexly coordinated regulatory network underlying the expression of *fimH* in *E. coli* O157: H7.

Given the key deletion in the switch region, together with our earlier observations that the presence of mannose had no influence on the adherence of SS isolates to RSE or other mammalian cells (Cote et al., 2015), we had not expected deletions in the *fim* operon to influence the adherence phenotype of *E. coli* O157. However, these preliminary investigations have defined an important role for *fim* in the adherence of some but not all *E. coli* O157 strains to specific mammalian cell types. This suggests the existence of a complex coordinately regulated network that contributes to the adherence phenotype of SS- *E. coli* O157 and other *E. coli* O157 strains in a lineage and host cell type dependent manner, and

therefore may be pathoadaptive. Furthermore, we were also able to verify the presence of type 1 fimbriae-like structures on wild type, Δ*fimH*, and Δ*fimH* complemented SS17 and EDL933 strains of *E. coli* O157 via negative and immunogold staining-based transmission electron microscopy. These structures could not be detected in the Δ*fimH* mutants of both SS17 and EDL933, indicating that these type 1-like fimbriae are probably expressed under controlled regulatory conditions explaining the phenotype observed.

It is well documented that bacteria respond to changes in their surrounding by altering the pattern of gene expression that is transcriptionally regulated (McAdams et al., 2004). A multitude of previous studies have been conducted to understand the genetic regulatory systems under a variety of genetic and environmental conditions, many of which have shown the existence of complex regulatory networks that synchronize the expression of a number of genes in prokaryotes (Donnenberg and Whittam, 2001; McVicker et al., 2011; Mizuno, 1997; Schwan, 2011; Schwan et al., 2002, 2007; Suzuki et al., 2002). For instance, it has been shown that in the *E. coli* K-12 genome, there are nearly 30 such complexly regulated two-component systems (Mizuno, 1997; Suzuki et al., 2002). In uropathogenic *E. coli*, a number of proteins have been shown to play roles in the expression of *fim* operon as well (Schwan, 2011; Schwan et al., 2002, 2007). However, it remains unknown whether the phenotypic changes observed in the current study may be attributed to the polar effects of the *fim* operon. Although the *fim* switch is off, minimal (below detection limits) read-through of *fimH* might still be occurring. Alternatively, it is possible that despite the *fim* switch being in the “off” position, the type 1 fimbrial locus may also encode genetic elements or contain binding sites for regulatory molecules such as enhancers, suppressors, and de-repressors, that act in concert to enable the coordinated regulation of the adhesion phenotype in some (but not all) *E. coli* O157 strains. Future studies will entail further analysis of the role of the individual genes of the fim operon, and detailed investigations of the functional consequences of these differences, if any, in contributing to the differences observed in adherence phenotypes in both supershedders and reference strains is needed.

Taken together, the results presented here suggest the existence of a similar complex regulatory underlying network that controls *E. coli* O157 adherence, including genetic elements located in the *fim* operon in a strain and host-cell dependent manner.

Supplementary Material

Refer to Web version on PubMed Central for supplementary material.

Acknowledgements

Excellent technical assistance provided by Bryan Wheeler at the National Animal Disease Center (NADC), Ames, IA, is gratefully acknowledged. The Animal Resource Unit personnel at NADC are also gratefully acknowledged for assisting with the collection of bovine rectoanal junction tissues and swabs for RSE cells.

Funding

V.K. was supported, in part, by the USDA National Institute of Food and Agriculture and Multistate/Regional Research and/or Extension Appropriations under Project #PEN04637 and Accession #1014673. This work was also supported by USDA-ARS CRIS projects 5030-32000-112-00D to I.T.K; and National Institute of Health, grant number AI143050 to E.V.S.

Mention of trade names or commercial products in this article is solely for providing specific information and does not imply recommendation or endorsement by the U.S. Department of Agriculture. USDA is an equal opportunity provider and employer.

References

Abraham SN, Goguen JD, Sun D, Klemm P, Beachey EH, 1987. Identification of two ancillary subunits of *Escherichia coli* type 1 fimbriae by using antibodies against synthetic oligopeptides of fim gene products. J. Bacteriol. 169 (12), 5530–5536. [PubMed: 2890622]

Arthur TM, Brichta-Harhay DM, Bosilevac JM, Kalchayanand N, Shackelford SD, Wheeler TL, et al. , 2010. Super-shedding of *Escherichia coli* O157:H7 by cattle and the impact on beef carcass contamination. Meat Sci. 86 (1), 32–37. [PubMed: 20627603]

Arthur TM, Ahmed R, Chase-Topping M, Kalchayanand N, Schmidt JW, Bono JL, 2013. Characterization of *Escherichia coli* O157:H7 strains isolated from supershedding cattle. Appl. Environ. Microbiol. 79 (14), 4294–4303. [PubMed: 23645203]

Brinton CC Jr., 1965. The structure, function, synthesis and genetic control of bacterial pili and a molecular model for DNA and RNA transport in gram negative bacteria. Trans. N. Y. Acad. Sci. 27 (8), 1003–1054. [PubMed: 5318403]

Burland V, Shao Y, Perna NT, Plunkett G, Sofia HJ, Blattner FR, 1998. The complete DNA sequence and analysis of the large virulence plasmid of *Escherichia coli* O157:H7. Nucleic Acids Res. 26 (18), 4196–4204. [PubMed: 9722640]

Centers for Disease Control and Prevention, 2011. Vital signs: incidence and trends of infection with pathogens transmitted commonly through food - foodborne diseases active surveillance network, 10 U.S. sites, 1996–2010. Morb. Mortal. Wkly. Rep. 60 (22), 729–772.

Cote R, Katani R, Moreau MR, Kudva IT, Arthur TM, DebRoy C, et al. , 2015. Comparative analysis of super-shedder strains of *Escherichia coli* O157:H7 reveals distinctive genomic features and a strongly aggregative adherent phenotype on bovine rectoanal junction squamous epithelial cells. PLoS One 10 (2), e0116743.

Datta S, Costantino N, Court DL, 2006. A set of recombineering plasmids for gram-negative bacteria. Gene 379, 109–115. [PubMed: 16750601]

Dewey-Mattia D, Manikonda K, Hall AJ, Wise ME, Crowe SJ, 2018. Surveillance for foodborne disease outbreaks — United States, 2009–2015. Mmwr Surveill. Summ. 67 (10), 1–11.

Donnenberg MS, Whittam TS, 2001. Pathogenesis and evolution of virulence in enteropathogenic and enterohemorrhagic *Escherichia coli*. J. Clin. Invest. 107 (5), 539–548. [PubMed: 11238553]

Eppinger M, Mammel MK, Leclerc JE, Ravel J, Cebula TA, 2011. Genomic anatomy of *Escherichia coli* O157:H7 outbreaks. Proc. Natl. Acad. Sci. U. S. A. 108 (50), 20142–20147. [PubMed: 22135463]

Farfan MJ, Cantero L, Vergara A, Vidal R, Torres AG, 2013. The long polar fimbriae of STEC O157:H7 induce expression of pro-inflammatory markers by intestinal epithelial cells. Vet. Immunol. Immunopathol. 152 (1–2), 126–131. [PubMed: 23078900]

Furukawa I, Suzuki M, Masaoka T, Nakajima N, Mitani E, Tasaka M, et al. , 2018. An outbreak of enterohemorrhagic *Escherichia coli* O157:H7 infection associated with minced meat cutlets in Kanagawa, Japan. Jpn. J. Infect. Dis, advpub

Gally DL, Bogan JA, Eisenstein BI, Blomfield IC, 1993. Environmental regulation of the fim switch controlling type 1 fimbrial phase variation in *Escherichia coli* K-12: effects of temperature and media. J. Bacteriol. 175 (19), 6186–6193. [PubMed: 8104927]

Garcia-Contreras R, Zhang XS, Kim Y, Wood TK, 2008. Protein translation and cell death: the role of rare tRNAs in biofilm formation and in activating dormant phage killer genes. PLoS One 3 (6), e2394.

Gyles CL, 2007. Shiga toxin-producing *Escherichia coli*: an overview. J. Anim. Sci. 85 (13), E45–62. [PubMed: 17085726]

Hanson MS, Hempel J, Brinton CC Jr., 1988. Purification of the *Escherichia coli* type 1 pilin and minor pilus proteins and partial characterization of the adhesin protein. J. Bacteriol. 170 (8), 3350–3358. [PubMed: 2900235]

Hayashi T, Makino K, Ohnishi M, Kurokawa K, Ishii K, Yokoyama K, et al. , 2001. Complete genome sequence of enterohemorrhagic *Escherichia coli* O157:H7 and genomic comparison with a laboratory strain K-12. DNA Res. 8 (1), 11–22. [PubMed: 11258796]

Iida K-I, Mizunoe Y, Wai SN, Yoshida S-I, 2001. Type 1 fimbriation and its phase switching in diarrheagenic *Escherichia coli* strains. Clin. Diagn. Lab. Immunol. 8 (3), 489–495. [PubMed: 11329445]

John M, Kudva IT, Griffin RW, Dodson AW, McManus B, Krastins B, et al. , 2005. Use of in vivo-induced antigen technology for identification of *Escherichia coli* O157:H7 proteins expressed during human infection. Infect. Immun. 73 (5), 2665–2679. [PubMed: 15845468]

Jordan DM, Cornick N, Torres AG, Dean-Nystrom EA, Kaper JB, Moon HW, 2004. Long polar fimbriae contribute to colonization by *Escherichia coli* O157:H7 in vivo. Infect. Immun. 72 (10), 6168–6171. [PubMed: 15385526]

Katani R, Cote R, Raygoza Garay JA, Li L, Arthur TM, DebRoy C, et al. , 2015. Complete genome sequence of SS52, a strain of Escherichia coli O157:H7 recovered from supershedder cattle. Genome Announc. 3 (2).

Katani R, Cote R, Kudva IT, DebRoy C, Arthur TM, Kapur V, 2017. Comparative genomics of two super-shedder isolates of Escherichia coli O157:H7. PLoS One 12 (8), e0182940.

Klemm P, 1984. The fimA gene encoding the type-1 fimbrial subunit of *Escherichia coli*. Nucleotide sequence and primary structure of the protein. Eur. J. Biochem. 143 (2), 395–399. [PubMed: 6147250]

Klemm P, Christiansen G, 1987. Three fim genes required for the regulation of length and mediation of adhesion of *Escherichia coli* type 1 fimbriae. Mol. Gen. Genet.: MGG 208 (3), 439–445. [PubMed: 2890081]

Kovach ME, Elzer PH, Hill DS, Robertson GT, Farris MA, Roop RM 2nd, et al. , 1995. Four new derivatives of the broad-host-range cloning vector pBBR1MCS, carrying different antibiotic-resistance cassettes. Gene 166 (1), 175–176. [PubMed: 8529885]

Kudva IT, Dean-Nystrom EA, 2011. Bovine recto-anal junction squamous epithelial (RSE) cell adhesion assay for studying Escherichia coli O157 adherence. J. Appl. Microbiol. 111 (5), 1283–1294. [PubMed: 21883734]

Kudva IT, Griffin RW, Krastins B, Sarracino DA, Calderwood SB, John M, 2012. Proteins other than the locus of enterocyte effacement-encoded proteins contribute to *Escherichia coli* O157:H7 adherence to bovine rectoanal junction stratified squamous epithelial cells. BMC Microbiol. 12, 103. [PubMed: 22691138]

Kudva IT, Carter MQ, Sharma VK, Stasko JA, Giron JA, 2017. Curli temper adherence of *Escherichia coli* O157:H7 to squamous epithelial cells from the bovine recto-anal junction in a strain-dependent manner. Appl. Environ. Microbiol. 83 (1).

Kulasekara BR, Jacobs M, Zhou Y, Wu Z, Sims E, Saenphimmachak C, et al. , 2009. Analysis of the genome of the *Escherichia coli* O157:H7 2006 spinach-associated outbreak isolate indicates candidate genes that may enhance virulence. Infect. Immun. 77 (9), 3713–3721. [PubMed: 19564389]

Li B, Koch WH, Cebula TA, 1997. Detection and characterization of the fimA gene of *Escherichia coli* O157:H7. Mol. Cell. Probes 11 (6), 397–406. [PubMed: 9500807]

Lim JY, Li J, Sheng H, Besser TE, Potter K, Hovde CJ, 2007. *Escherichia coli* O157:H7 colonization at the rectoanal junction of long-duration culture-positive cattle. Appl. Environ. Microbiol. 73 (4), 1380–1382. [PubMed: 17189448]

Lloyd SJ, Ritchie JM, Rojas-Lopez M, Blumentritt CA, Popov VL, Greenwich JL, et al. , 2012. A double, long polar fimbria mutant of *Escherichia coli* O157:H7 expresses Curli and exhibits reduced in vivo colonization. Infect. Immun. 80 (3), 914–920. [PubMed: 22232190]

Matthews L, Low JC, Gally DL, Pearce MC, Mellor DJ, Heesterbeek JAP, et al. , 2006. Heterogeneous shedding of *Escherichia coli* O157 in cattle and its implications for control. Proc. Natl. Acad. Sci. U. S. A. 103 (3), 547–552. [PubMed: 16407143]

McAdams HH, Srinivasan B, Arkin AP, 2004. The evolution of genetic regulatory systems in bacteria. Nat. Rev. Genet. 5 (3), 169–178. [PubMed: 14970819]

McVicker G, Sun L, Sohanpal BK, Gashi K, Williamson RA, Plumbridge J, et al. , 2011. SlyA protein activates fimB gene expression and type 1 fimbriation in *Escherichia coli* K-12. J. Biol. Chem. 286 (37), 32026–32035. [PubMed: 21768111]

Mikhail AFW, Jenkins C, Dallman TJ, Inns T, Douglas A, MartÍN AIC, et al. , 2018. An outbreak of Shiga toxin-producing *Escherichia coli* O157:H7 associated with contaminated salad leaves: epidemiological, genomic and food trace back investigations. Epidemiol. Infect. 146 (2), 187–196. [PubMed: 29248018]

Mizuno T, 1997. Compilation of all genes encoding two-component phosphotransfer signal transducers in the genome of *Escherichia coli*. DNA Res. 4 (2), 161–168. [PubMed: 9205844]

Nataro JP, Kaper JB, 1998. Diarrheagenic Escherichia coli. Clin. Microbiol. Rev. 11 (1), 142–201. [PubMed: 9457432]

Naylor SW, Low JC, Besser TE, Mahajan A, Gunn GJ, Pearce MC, et al. , 2003. Lymphoid follicle-dense mucosa at the terminal rectum is the principal site of colonization of enterohemorrhagic *Escherichia coli* O157:H7 in the bovine host. Infect. Immun. 71 (3), 1505–1512. [PubMed: 12595469]

Omisakin F, MacRae M, Ogden ID, Strachan NJC, 2003. Concentration and prevalence of *Escherichia coli* O157 in cattle feces at slaughter. Appl. Environ. Microbiol. 69 (5), 2444–2447. [PubMed: 12732509]

Paton JC, Paton AW, 1998. Pathogenesis and diagnosis of shiga toxin-producing *Escherichia coli* infections. Clin. Microbiol. Rev. 11 (3), 450–479. [PubMed: 9665978]

Perna NT, Plunkett G, Burland V, Mau B, Glasner JD, Rose DJ, et al. , 2001a. Genome sequence of enterohaemorrhagic *Escherichia coli* O157:H7. Nature 409 (6819), 529–533. [PubMed: 11206551]

Perna NT, Plunkett G 3rd, Burland V, Mau B, Glasner JD, Rose DJ, et al. , 2001b. Genome sequence of enterohaemorrhagic *Escherichia coli* O157:H7. Nature 409 (6819), 529–533. [PubMed: 11206551]

PulseNet. Centers for Disease Control and Prevention- PulseNet Centers for Disease Control and Prevention 2013 [01/14/2015]. Available from: http://www.cdc.gov/pulsenet/.

Roe AJ, Currie C, Smith DG, Gally DL, 2001. Analysis of type 1 fimbriae expression in verotoxigenic *Escherichia coli*: a comparison between serotypes O157 and O26. Microbiology 147 (Pt 1), 145–152. [PubMed: 11160808]

Scallan E, Hoekstra RM, Angulo FJ, Tauxe RV, Widdowson MA, Roy SL, et al. , 2011. Foodborne illness acquired in the United States–major pathogens. Emerging Infect. Dis. 17 (1), 7–15.

Schwan WR, 2011. Regulation of fim genes in uropathogenic *Escherichia coli*. World J. Clin. Infect. Dis. 1 (1), 17–25.

Schwan WR, Lee JL, Lenard FA, Matthews BT, Beck MT, 2002. Osmolarity and pH growth conditions regulate fim gene transcription and type 1 pilus expression in uropathogenic *Escherichia coli*. Infect. Immun. 70 (3), 1391–1402. [PubMed: 11854225]

Schwan WR, Shibata S, Aizawa S, Wolfe AJ, 2007. The two-component response regulator RcsB regulates type 1 piliation in *Escherichia coli*. J. Bacteriol. 189 (19), 7159–7163. [PubMed: 17644608]

Shaikh N, Holt NJ, Johnson JR, Tarr PI, 2007. Fim operon variation in the emergence of Enterohemorrhagic *Escherichia coli*: an evolutionary and functional analysis. FEMS Microbiol. Lett. 273 (1), 58–63. [PubMed: 17559392]

Sokurenko EV, Courtney HS, Abraham SN, Klemm P, Hasty DL, 1992. Functional heterogeneity of type 1 fimbriae of *Escherichia coli*. Infect. Immun. 60 (11), 4709–4719. [PubMed: 1356930]

Sokurenko EV, Courtney HS, Ohman DE, Klemm P, Hasty DL, 1994. FimH family of type 1 fimbrial adhesins: functional heterogeneity due to minor sequence variations among fimH genes. J. Bacteriol. 176 (3), 748–755. [PubMed: 7905476]

Sokurenko EV, Chesnokova V, Dykhuizen DE, Ofek I, Wu XR, Krogfelt KA, et al. , 1998. Pathogenic adaptation of *Escherichia coli* by natural variation of the FimH adhesin. Proc. Natl. Acad. Sci. U. S. A. 95 (15), 8922–8926. [PubMed: 9671780]

Stevens MP, van Diemen PM, Dziva F, Jones PW, Wallis TS, 2002. Options for the control of enterohaemorrhagic *Escherichia coli* in ruminants. Microbiology 148 (Pt 12), 3767–3778. [PubMed: 12480881]

Stirling JW, Graff PS, 1995. Antigen unmasking for immunoelectron microscopy: labeling is improved by treating with sodium ethoxide or sodium metaperiodate, then heating on retrieval medium. J. Histochem. Cytochem. 43 (2), 115–123. [PubMed: 7529784]

Suzuki K, Wang X, Weilbacher T, Pernestig AK, Melefors O, Georgellis D, et al. , 2002. Regulatory circuitry of the CsrA/CsrB and BarA/UvrY systems of *Escherichia coli*. J. Bacteriol. 184 (18), 5130–5140. [PubMed: 12193630]

Tamminen L-M, Fransson H, Tråvén M, Aspán A, Alenius S, Emanuelson U, et al. , 2018. Effect of on-farm interventions in the aftermath of an outbreak of hypervirulent verocytotoxin-producing Escherichia coli O157:H7 in Sweden. Vet. Rec. 182 (18), 5130–5140.

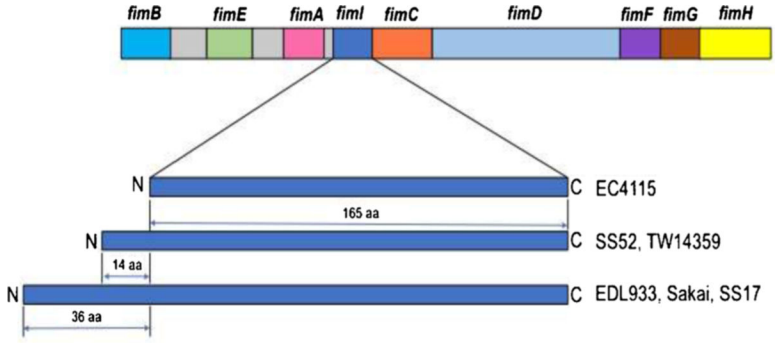

Fig. 1. Comparative genomic analysis of the *fimI* gene between different strains of *E. coli* O157.
The type 1 *fim* operon is represented with color-coded gene regions. The *fimI* gene, represented in the dark blue color, varies in length between the different strains, as represented in the enlarged portion of the figure.

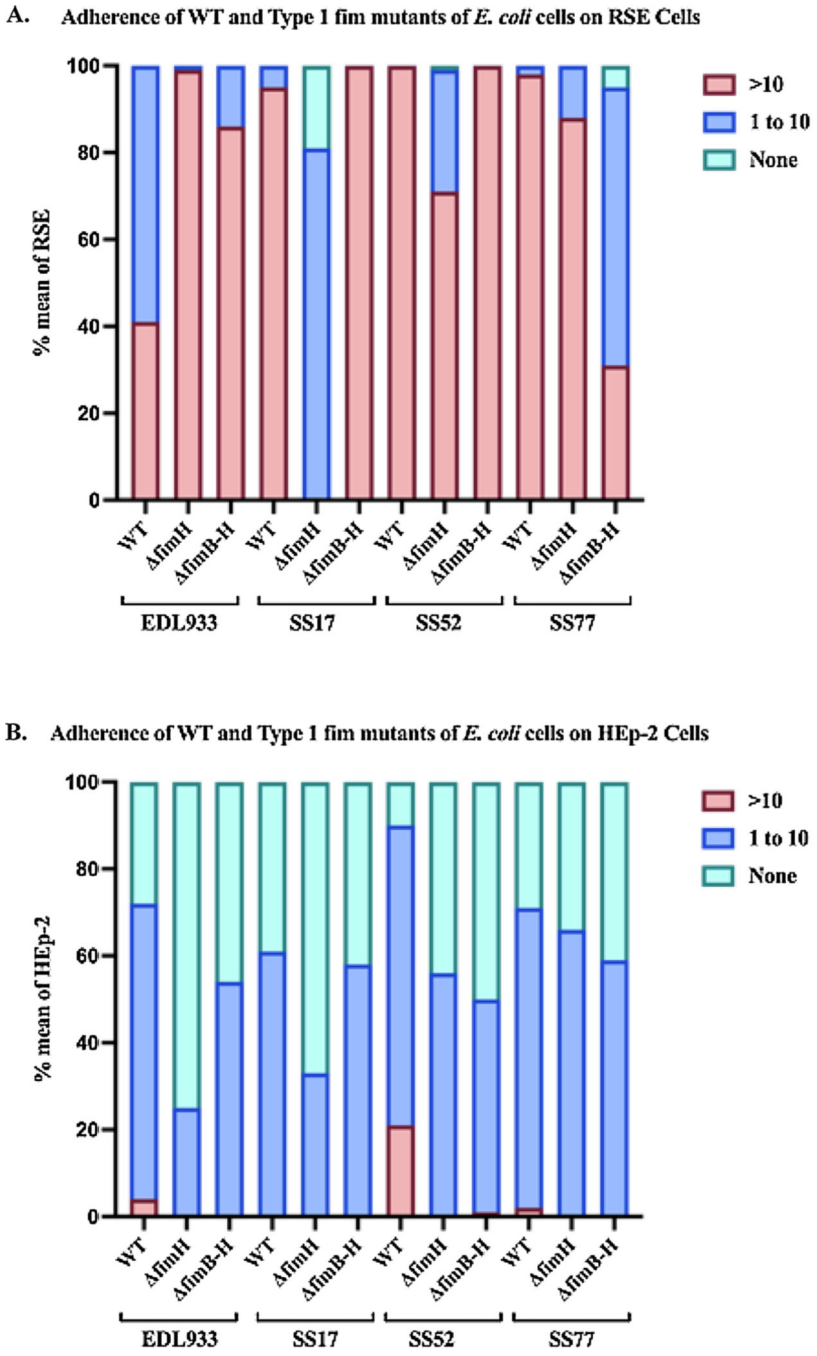

Fig. 2. The mean percentage of epithelial cells (RSE and HEp-2 cells) with >10, 1–10, and none of *E. coli* O157 cells adherance is shown for WT and fim Type 1 mutant (ΔfimH and ΔfimB-H) strains of *E. coli* O157 strains.

A) RSE cells, **B)** HEp-2 cells. Each trial had one slide per bacterial group. Each slide had 4 spots/chambers (technical replicate) on it; 10–20 well-dispersed cells were evaluated per spot/chamber. The details of the percent Mean +/− standard error (SEM) of the eukaryotic cells with adherent bacteria are shown in supplemental Tables S4 (RSE) and S5 (HEp-2) cells.

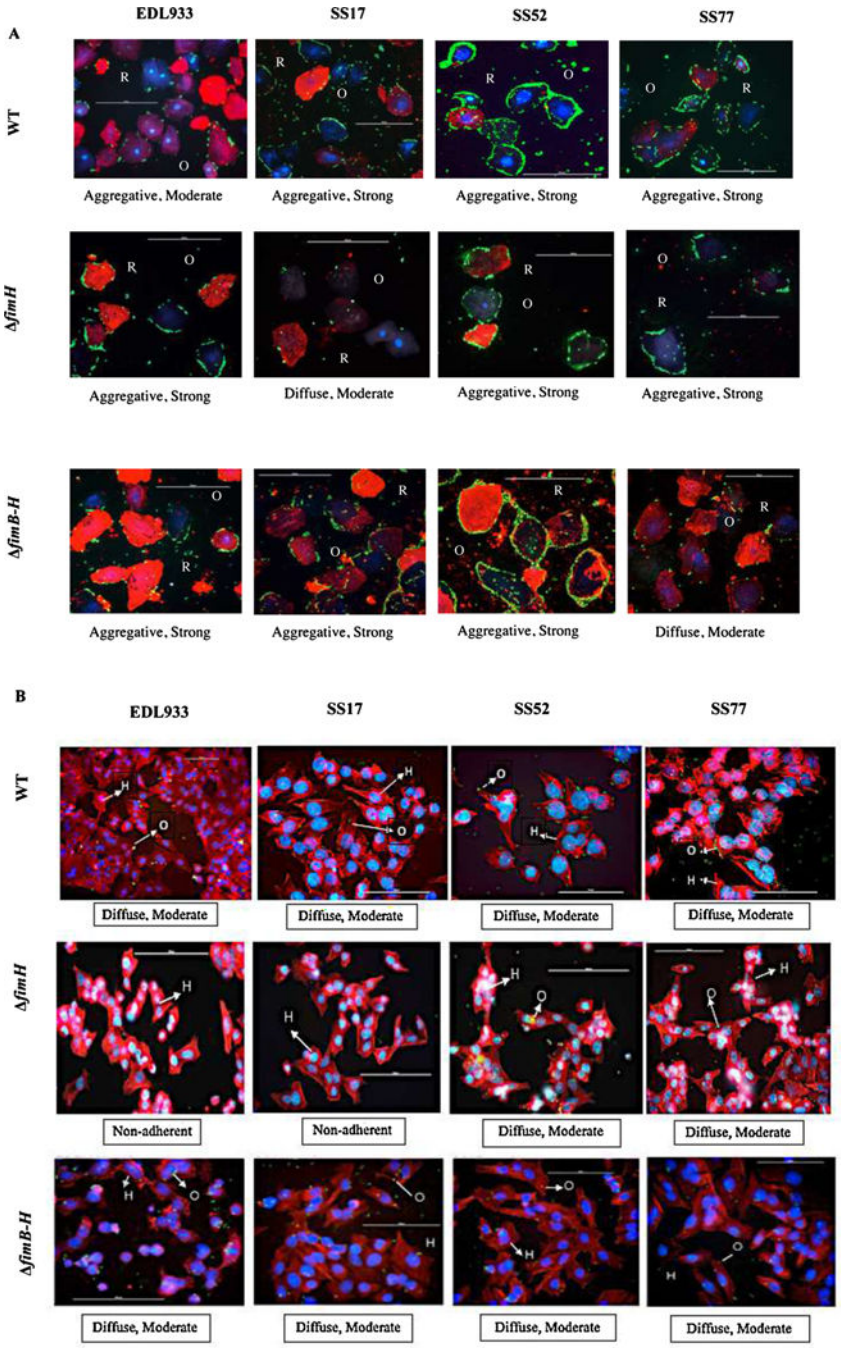

Fig. 3. Adherence images of mutant *E. coli* O157 strains on A) RSE and B) HEp-2 cells.

The figure indicates heterogeneity between EDL933 and SS- *E. coli* O157. Mutant strains of *E. coli* O157 with SS17Δ*fimH* and SS77Δ*fimB-H* manifest a diffuse and moderate adherence to the RSE cells, a decrease of the aggregative and strong phenotype observed in the parental SS strains. Both EDL933 mutants manifested an increase in the adherence to the RSE cells. The immunofluorescence-stained slides are shown at 40x magnification with RSE cells and 20x magnification with HEp-2 cells. Bacteria (*E. coli* O157) have green fluorescence, RSE cells' cytokeratins and HEp-2 cells' actin filaments have orange-red

fluorescence, and the nuclei of both cells have blue fluorescence. R, RSE cell; O, *E. coli* O157; H, HEp-2 cell.

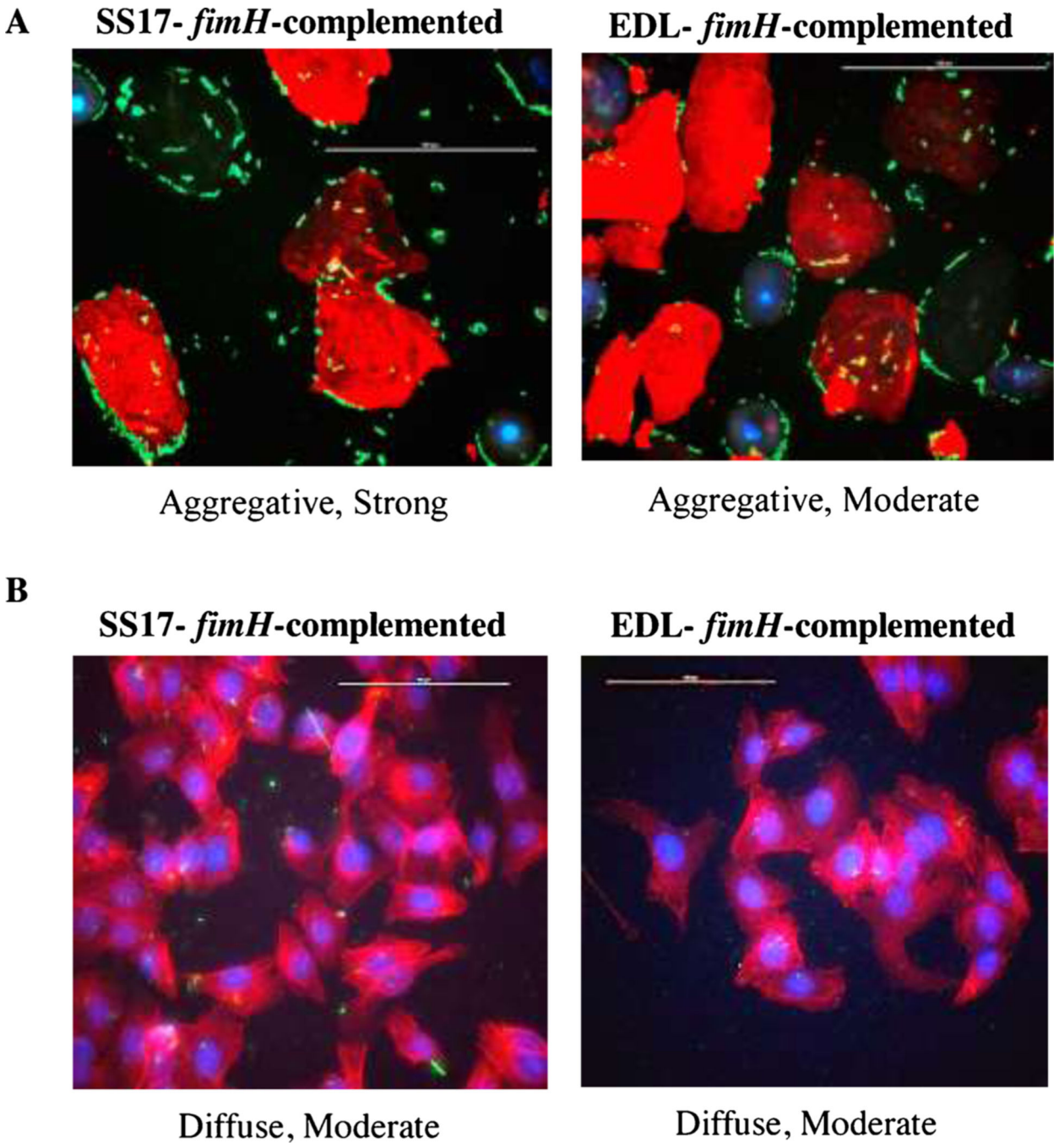

Fig. 4. Adherence images of *fimH*-complemented strains of SS17 and EDL933 to A) RSE and B) HEp-2 cells.

When *fimH* is complemented, both SS17 and EDL933 revert back to their respective WT adherence phenotype on both RSE (aggregative, strong in SS17 and aggregative, moderate in EDL933), and HEp-2 cells (diffuse, moderate in both SS17 and EDL933). Slides are shown at 40x magnification with RSE cells and 20x magnification with HEp-2 cells. Bacteria (*E. coli* O157) have green fluorescence, RSE cells' cytokeratins and HEp-2 cells' actin filaments have orange-red fluorescence, and the nuclei of both cells have blue fluorescence.

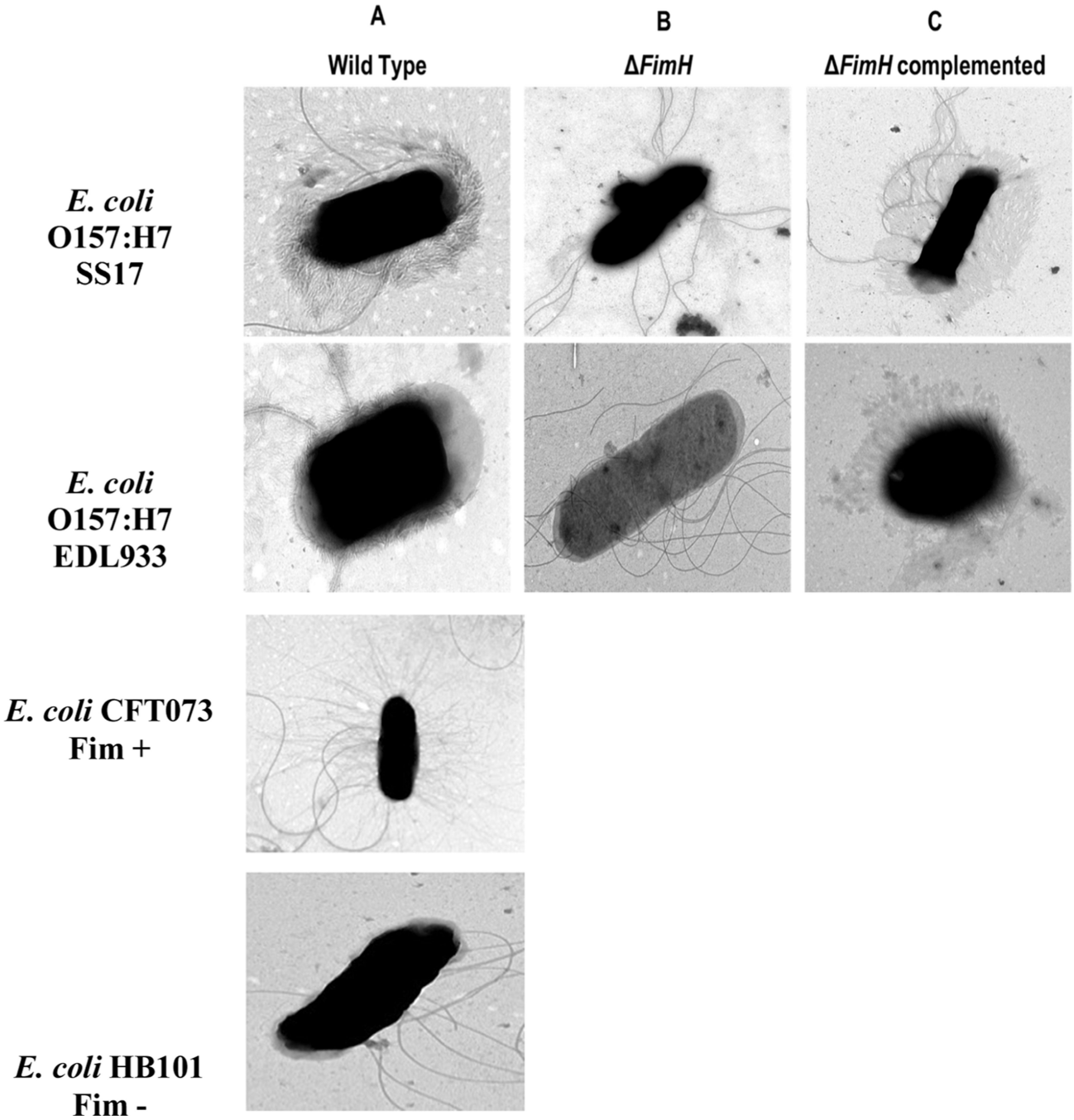

Fig. 5. Negatively stained TEM micrographs of A) wild type; B) Δ*fimH;* C) Δ*fimH*-complemented *E. coli* O157 strains SS17 and EDL933.

Wild type UPEC CFT073 and *E. coli* HB101 were used as positive and negative controls, respectively. Type 1 fimbriae-like structures are seen in the wild type and in complemented *E. coli* O157 strains SS17 and EDL933. These structures vary from the typical type 1 fimbriae seen in *E. coli* CFT073 used as a positive control. Direct magnification: 13,000x to 49,000 ×.

A. ***E. coli*** **CFT073 (Fim +)**

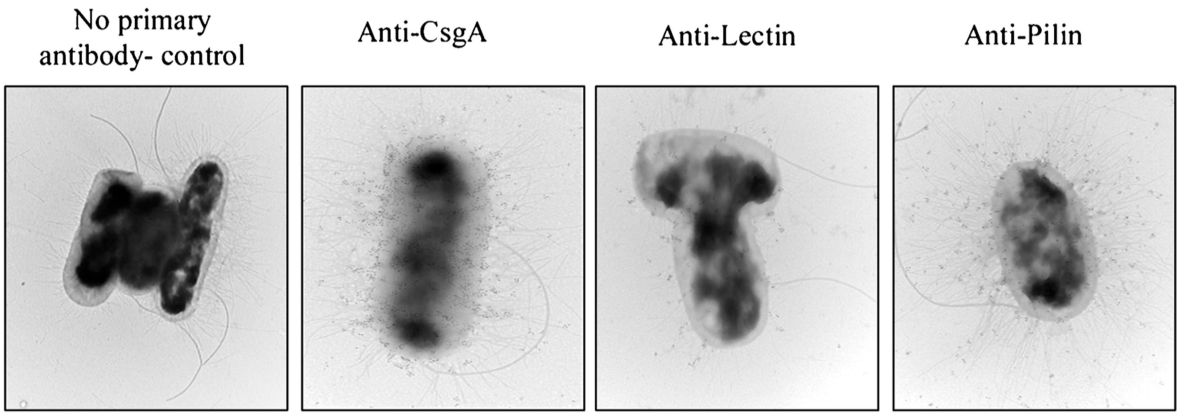

B. ***E. coli*** **HB101 (Fim -)**

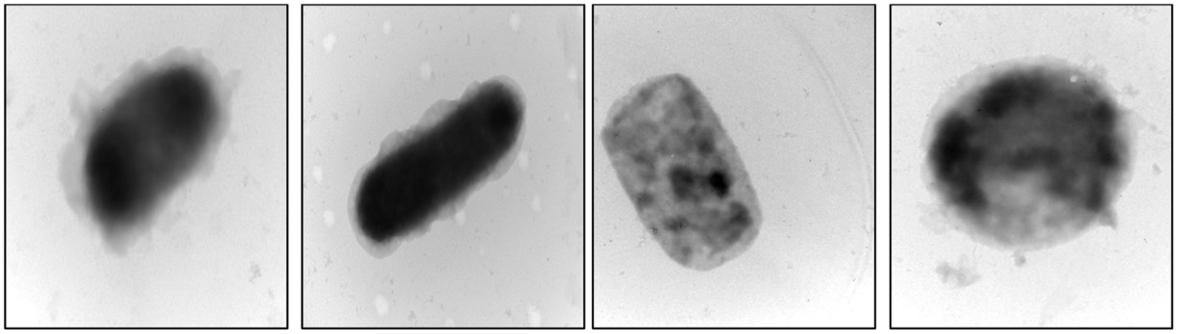

Fig. 6. Immunogold stained electron micrographs of type 1 fimbrial structures in (A) UPEC CFT073 and (B) *E. coli* HB101

used as positive and negative controls, respectively. Direct Magnification: 30,000×.

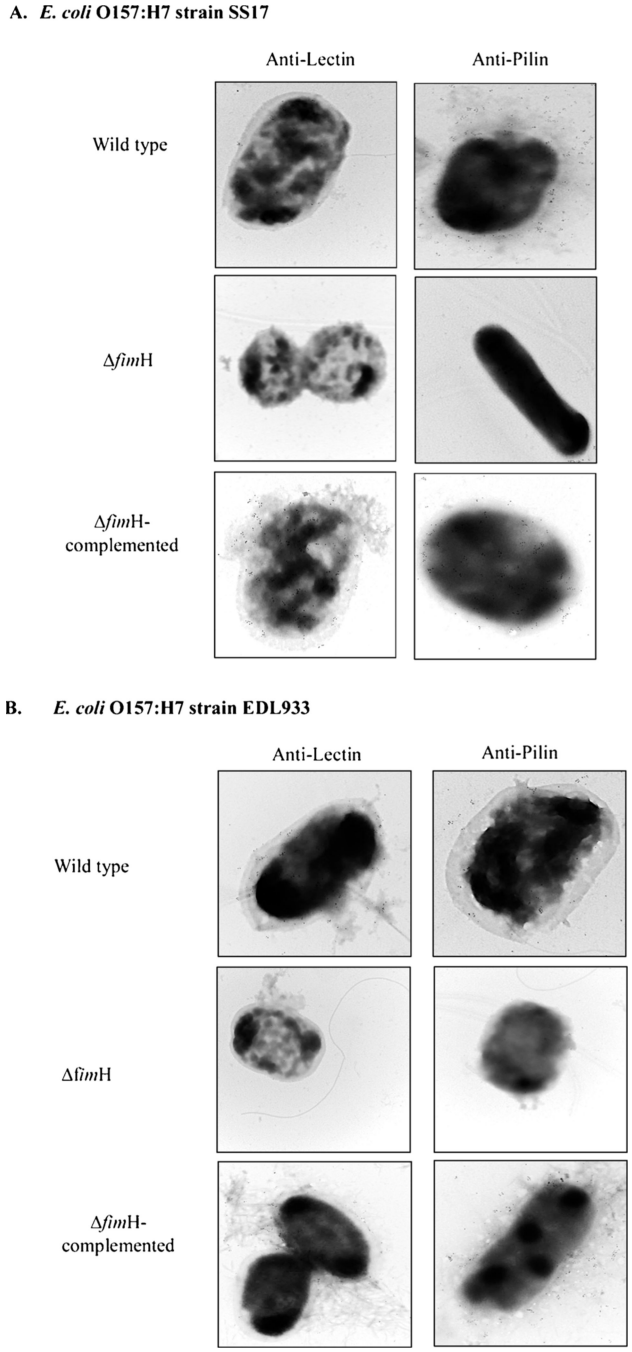

Fig. 7. Immunogold stained electron micrographs of type 1 fimbriae-like structures in wild type, Δ*fimH* and Δ*fimH* complemented *E. coli* O157 strains (A) SS17 and (B) EDL933.
Direct magnification: 30,000×.

Table 1

Comparative analysis of the *fim* operon in SS52 and *E. coli* O157 reference strains.

O157 Strains	*fim* operon								
	fimB	***fimE***	***fimA***	***fimI***	***fimC***	***fimD***	***fimF***	***fimG***	***fimH***
EC4115	-	V1M	-	165aa	V1M	-	-	-	-
EDL933	-	V1M	-	215aa	V1M	-	-	-	N135K
Sakai	-	V1M	A100V	215aa	V1M	-	-	-	N135K
SS17	-	V1M	-	215aa	V1M	-	-	-	-
TW14359	P80S	V1M	-	-	V1M	-	-	-	-

Int J Med Microbiol. Author manuscript; available in PMC 2021 November 20.